TRANSACTIONS OF THE INSTITUTE OF FLUID-FLOW MACHINERY

No. 128, 2015, 29–42

ALEKSANDRA ROSZKO[1] and ELŻBIETA FORNALIK-WAJS

The heat transfer and flow structure analyses of low concentration copper nanofluids in a strong magnetic field

AGH University of Science and Technology, Department of Fundamental Research in Energy Engineering, Mickiewicza 30, 30-059 Cracow, Poland

Abstract

Main aim of this paper was to analyze the influence of strong magnetic field on the enhancement or suppression of nanofluids transport processes. The second objective was to determine how the flow structure changed under the influence of a magnetic field. Analyzed diamagnetic nanofluids composed of distilled water and the copper nanoparticles of 40–60 nm size in three different concentrations (50, 500, and 1000 ppm). The experimental enclosure position in the magnet test section caused the most intricate interaction of the acting forces: the gravitational and magnetic buoyancy ones, and made the interpretation of results very difficult. The Nusselt number ratio and the thermomagnetic Rayleigh number were determined for heat transfer analysis, while the fast Fourier transform was performed for the nanofluid flow structure analysis. Spectral analysis for all examined nanofluids was presented. Influence of nanoparticles concentration was clearly visible, while the direct impact of magnetic field on the heat transfer and flow structure should be still investigated.

Keywords: Nanofluids; Heat transfer; Flow structure; Fast Fourier transform; Nusselt number ratio; Thermomagnetic Rayleigh number

Nomenclature

$\mathbf{B}$	–	magnetic induction, T
c_p	–	specific heat, $\mathrm{J(kg\,K)^{-1}}$

[1]Corresponding Author. E-mail address: roszko@agh.edu.pl

$\mathbf{F}$ – force, $\mathrm{N m^{-3}}$
$\mathbf{g}$ – gravitational acceleration, $\mathrm{m s^{-2}}$
k – thermal conductivity, $W(m\,K)^{-2}$
Q_{cond} – conduction heat rate, W
Q_{conv} – convective heat rate, W
Nu – Nusselt number, –
T – temperature, K
T_0 – reference temperature, K

Greek symbols

β – thermal expansion coefficient, $\mathrm{K^{-1}}$
φ – particle fraction, vol%
ρ – density, $\mathrm{kg\,m^{-3}}$
ρ_0 – density at reference temperature, $\mathrm{kg\,m^{-3}}$
μ – dynamic viscosity, $\mathrm{kg(m\,s)^{-1}}$
μ_0 – magnetic permeability of vacuum, $\mathrm{H\,m^{-1}}$
σ – electrical conductivity, $\mathrm{S\,m^{-1}}$
χ – mass magnetic susceptibility, $\mathrm{m^3\,kg^{-1}}$

Superscripts

bf – base fluid
g – gravitational
m – magnetic
nf – nanofluid
p – particles

1 Introduction

In recent years the nanofluids have gained attention due to their wide possible applications such as in cooling of electronic systems or thermal storage systems [1]. A large number of both experimental and numerical investigations were published in the past few decades, among them, the natural convection was considered in [2–4]. Change of the fluid properties caused by an addition of the nanoparticles was the subject of many reports [3,5,6]. Higher thermal properties and enhancement of heat transfer were presented by large number of research groups [7–9]. Few numerical calculations of weakly-magnetic nanofluids placed in a magnetic field was performed [10–12]. However, till now only one experimental diamagnetic nanofluids heat transfer investigations was accomplished [13].

One of the methods to obtain high heat fluxes transfer is an addition of the nanoparticles to the traditional coolants. The homogeneous coolants have limitations coming from their pretty low thermal properties. The second method is to utilized the magnetic field to enhance the thermal trans-

port processes. It was proved that such effect could be achieved for diamagnetic and paramagnetic, but one-phase, fluids [14,15]. In presented paper this two combined ways of heat transfer control were applied. The Nusselt number ratio was calculated and it helped to define occuring phenomena. The fast Fourier transform (FFT) and spectral analysis were applied to find information about the flow structure without and with influence of the magnetic field.

2 Experimental equipment

Schematic view of experimental equipment is shown in Fig. 1a. The experimental enclosure was filled with working nanofluid. Position of the cubical enclosure inside the test section of superconducting magnet was correlated with appearance of maximal value of grad$\mathbf{B}^2_{\max}$, which means that the magnetic buoyancy force has had the greatest impact at this point [14]. The bottom wall of experimental enclosure was heated (with constant heat flux) and the top one was cooled, both of them were made of copper. A nichrome wire was used as a heater, connected to a DC power supply and placed under cooper plate. The heating power was monitored with multimeters. The water flowing through the cooling chamber was maintained at constant temperature by a thermostating bath. Three thermocouples were placed in heated and cooled plates, while six thermocouples inside cubical enclosure (shown in Fig. 1b). The signals of measured temperature were stored in a computer memory through a data acquisition system and were used to analyze the heat transfer and flow structure.

2.1 Working fluids

The nanofluids consisted of the base fluid (distilled water) and copper particles (40–60 nm) of three concentrations were examined. The amount of nanoparticles were 50, 500 and 1000 ppm, it corresponded to following nomenclatures: Cu50, Cu500 and Cu1000, respectively. Preparation of nanofluids is very problematic and complicated [16]. The working nanofluids were prepared by two-step method based on the mechanical agitation during 8 h. The fluids were opaque but after one hour of stagnation, agglomeration and sedimentation were observed. The way of nanofluids preparation were improved in the next research steps.

The necessary (physical and thermal) properties for the heat transfer

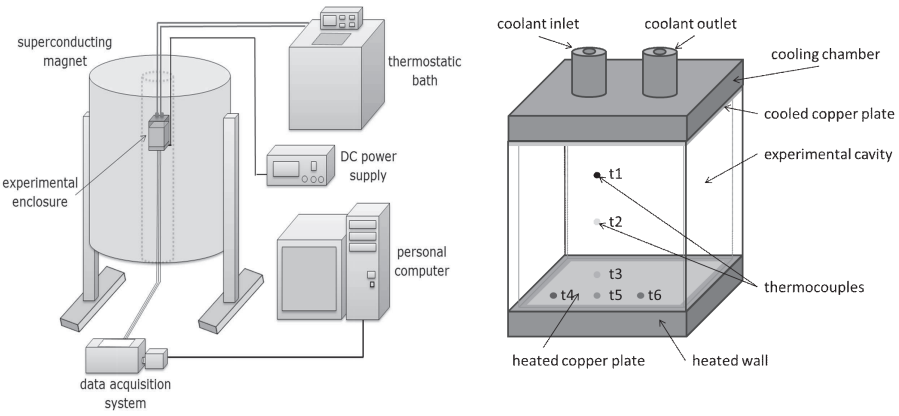

Figure 1: Experimental (a) setup and (b) enclosure.

and flow structure analyzes were calculated using formulas presented in Tab. 1. The magnetic properties were measured with the magnetic susceptibility balance (MSB Magnetic Susceptibility Balance, Sherwood Scientific Ltd. described in Operator's Manual). All working fluids' properties used in the analysis are presented in Tab. 2.

Table 1: Formulas applied for the calculation of nanofluids thermophysical properties [17].

Property	Formula
Thermal conductivity	$k_{nf} = k_{bf} \frac{k_p + 2k_{bf} + 2\varphi(k_p - k_{bf})}{k_p + 2k_{bf} - \varphi(k_p - k_{bf})}$
Density and specific heat product	$\rho c_{p,nf} = \varphi(\rho c_p)_p + (1-\varphi)(\rho c_p)_{bf}$
Thermal expansion coefficient	$\beta_{nf} = \varphi\beta_p + (1-\varphi)\beta_{bf}$
Dynamic viscosity	$\mu_{nf} = \frac{\mu_{bf}}{(1-\varphi)^{2.5}}$
Electrical conductivity	$\sigma_{nf} = \sigma_{bf}\left[1 + \frac{3\left(\frac{\sigma_p}{\sigma_{bf}} - 1\right)\varphi}{\left(\frac{\sigma_p}{\sigma_{bf}} + 2\right) - \left(\frac{\sigma_p}{\sigma_{bf}} - 1\right)\varphi}\right]$

Considering the magnetic properties of analysed fluids, it should be emphasized that both of the nanofluids components (water and copper) were

Table 2: Thermophysical properties of working fluids.

Property	Unit	Cu50* (50 ppm)	Cu500* (500 ppm)	Cu1000* (1000 ppm)
Thermal conductivity, k_{nf}	$\mathrm{W(mK)^{-1}}$	0.5990	0.5991	0.5992
Density, ρ_{nf}	$\mathrm{kg\,m^{-3}}$	1010.04	1010.44	1010.89
Specific heat, $c_{p,nf}$	$\mathrm{J\,(kg\,K)^{-1}}$	4181.78	4181.58	4181.58
Thermal expansion coefficient, β_{nf}	$\mathrm{K^{-1}}$	19.8×10^{-5}	19.8×10^{-5}	19.8×10^{-5}
Dynamic viscosity, μ_{nf}	$\mathrm{kg\,(m\,s)^{-1}}$	101.0×10^{-5}	101.0×10^{-5}	101.0×10^{-5}
Electrical conductivity, σ_{nf}	$\mathrm{S\,m^{-1}}$	5.50×10^{-6}	5.50×10^{-6}	5.50×10^{-6}
Mass magnetic susceptibility, χ_m	$\mathrm{m^3\,kg^{-1}}$	-13.4×10^{-9}**	-13.4×10^{-9}**	-14.5×10^{-9}**

* – values calculated in the basis of Tab. 1, ** – measured values.

diamagnetic. The selected fluids were considered as nonconducting electrical current, based on [18], thus the only acting forces were the gravitational and magnetic buoyancy forces.

2.2 The resultant forces

The force acting on the fluid is a sum of the gravitational and magnetic buoyancy forces. Mutual interaction of them affected the behavior and flow structure of the fluid. Its graphical interpretation is presented in Fig. 2.

Their values depended on many factors, i.e., physical, thermal (and magnetic) properties of the fluids. The gravitational buoyancy force can be described by following equation:

$$\mathbf{F}_g = \mathbf{g}\rho_0\beta(T - T_0)\ , \tag{1}$$

where ρ_0 is the density at reference temperature, whereas the magnetic buoyancy force for diamagnetics by formula

$$\mathbf{F}_m = \frac{\chi_m \rho_0 \beta (T - T_0)}{2\mu_0} \nabla \mathbf{B}^2_{max}\ , \tag{2}$$

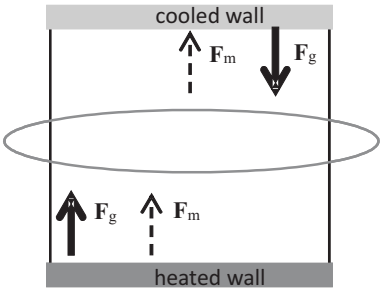

Figure 2: Reciprocal relation of the gravitational, $\mathbf{F}_g$, and magnetic, $\mathbf{F}_m$, buoyancy forces.

where the T_0 indicated reference temperature equal to the arithmetical average of cooled and heated walls temperature.

The gravitational buoyancy force on the hot fluid was acting upward, while on the cold downward. The magnetic buoyancy force described by Eq. (2) on the hot fluid was acting toward the maximal grad$\mathbf{B}^2_{\max}$, while on the cold fluid in opposite direction. This complex system of forces resulted in ambiguous fluid flow. In the lower part of the enclosure gravitational and magnetic buoyancy forces were strengthening each other, whereas in the upper part weakening.

The calculations of the forces acting on the fluid, were performed. Their ratio depended only on the fluid magnetic susceptibility, gravitational acceleration, magnetic permeability of vacuum, and the maximal gradient of magnetic induction square. For Cu50 and Cu500 the forces ratio was about 0.42, what means that the magnetic buoyancy force was 42% smaller than the gravitational one. Equal results for these fluids came from almost the same values of their magnetic susceptibility. For Cu1000 the ratio was about 0.45 – the magnetic buoyancy force slightly increased due to increase in the magnetic susceptibility of this fluid. Addition of copper particles (diamagnetic) caused increase of nanofluid absolute value of magnetic properties. Under studied conditions still the gravitational buoyancy force dominated in the enclosure, however the influence of magnetic field could be observed in Figs. 3–5.

3 Steps of the analysis

For each of nanofluids the procedure of the heat transfer and fluid flow analysis was the same. The first stage was connected with an analysis of

conduction state. It was necessary for determination of the Nusselt number defined as

$$\mathrm{Nu} = \frac{Q_{conv}}{Q_{cond}}\,, \tag{3}$$

and also for the heat losses as substantial for the heat transfer. For this stage the experimental enclosure was turned upside-down. The calculation details can be found in [13]. Afterward the analysis of pure thermal and thermomagnetic convections were conducted for all nanofluids. The enclosure was again in the position presented in Fig. 1b. Pure thermal convection was analysed as the reference state for estimation of magnetic field impact. The magnetic induction was then changed stepwisely from 2 to 9 T. After each step the time needed to stabilize the system was about 1–2 h. The results are presented in the form of Nusselt number ratio to emphasize the magnetic field influence. The ratio was calculated as division between value of Nusselt number under the influence of magnetic field and the Nusselt number for pure natural convection (without magnetic field). The same way of data presenting was applied to the convective and conduction heat rates ratio.

3.1 Results and discussion

In Fig. 3a the results of heat transfer analysis are represented by ratio between the Nusselt number with and without the magnetic field and thermomagnetic Rayleigh number dependence. The values of Nusselt number ratio for Cu50 decreased with increasing magnetic induction, what corresponded to the suppression of convection as the result of counteracting magnetic and gravitational buoyancy forces. For Cu500 the magnetic field influence was very weak, therefore after slight increase at 4 T of magnetic induction the results were almost constant. The strongest effect of magnetic field on the fluid behaviour could be observed for Cu1000, for which the Nusselt number ratio increased about 25%. To understand deeply the influence of nanofluids' properties changes on the heat transfer, the convective and conduction heat rates ratios were shown in Fig. 3b and 3c. With increasing magnetic induction the convective heat rate ratios for Cu50 and Cu500 didn't change much, whereas for Cu1000 it increased slightly up to 8 T, than the ratio value felled slightly at 9 T for Cu50 and Cu1000. The difference between the Cu50, Cu500, and Cu1000 are probably coming from their physical properties, even the changes are not very clear. The conduction heat rate ratio (Fig. 3c) took the lowest value for Cu1000. Slight increase of conduction heat rate ratio for Cu50 with increasing magnetic induction could be ob-

served, while for Cu500 it stand almost constant. The probable explanation is connected with higher magnetic field impact on the Cu1000 convection.

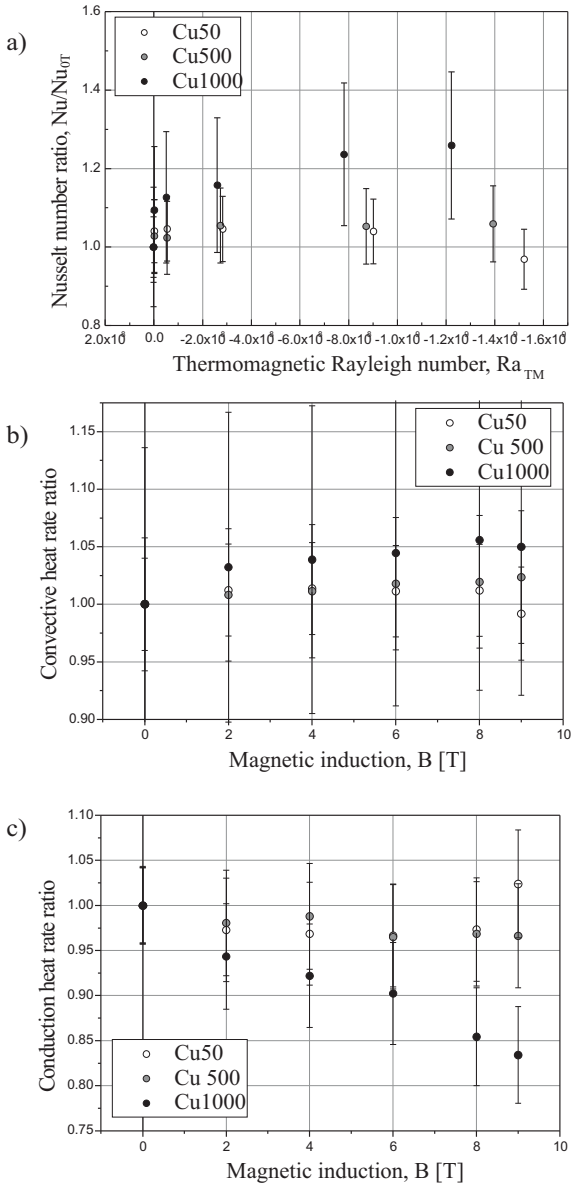

Figure 3: (a) The Nusselt number ratio versus the thermomagnetic Rayleigh number; (b) convective and (c) conduction heat rates ratios depended on the magnetic induction.

Examples of spectral analysis at 0 T for Cu50, Cu500 and Cu1000, also log-log scale diagrams for all nanofluids are presented in Fig. 4, respectively. The abbreviations t1-t6 represent recorded signals from the thermocouples shown in Fig. 1(b). Dependence of power density on frequency was calculated using FFT analysis, by the time-integral squared amplitude (TISA) method. Generally temperature spectral functions generally depends on the energy dissipation, temperature, kinematic viscosity and thermal diffusivity. In the inertial-convective range, the spectra do not depend on the diffusion processes, therefore do not depend on the kinematic viscosity or thermal diffusivity. The function is similar to the energy spectrum as the power function of wave number with exponent -5/3. When, the thermal diffusivity becomes more significant, the range is called viscous-diffusive and the spectral function is proportional to the inverse value of wave number (k^{-1}) [20]. The straight lines with slopes of -5/3 and 1 were shown in Figs. 4 and 5 to find the analogy between theory and experiment. One clear peak was visible on the Cu1000 diagram and its magnitude was smaller at 9 T, which is presented in Fig. 5. There were many peaks representing flow structures for Cu50 and Cu500 at 0 T, and their magnitutes were also smaller at 9 T of magnetic induction, see Fig. 5. It could indicate a suppression of thermomagnetic convection. It looked like the number and strength of vortices were reduced, so the magnetic field changed the flow structure and also energy transported by them. As it was mentioned earlier due to the complex forces system, the unequivocal interpretation of results is difficult.

The power spectrum representations in log-log scale for Cu50, Cu500 and Cu1000 at 0 T are shown in Fig. 4. The straight solid line of -5/3 slope was in good agreement with the power spectrum for Cu500 and Cu1000, what suggested the flow occurring in the inertial-convective turbulent regime [19]. The flow characteristics for Cu50 did not fit in this range. The straight dotted line of -1 slope did not match the power spectrum distribution in any range for any fluid. The power spectrum representations in log-log scale for Cu50, Cu500 and Cu1000 at 9 T was presented in Fig. 5, by analogy. The straight lines (-5/3 and -1 slopes) Cu50, Cu500 did not match these flow regimes. However pretty good agreement with Cu1000 could be observed, the change in nanofluids flow structure was noticeable.

The peaks, in spectral analysis, indicated occurrence of a certain periodicity, shown in Figs. 4 and 5. Therefore, the peaks could be identified with the existing vortices of determined frequency and their manual 'visualization' was performed. The peaks, which were characterized by the same

frequency, at the same time for various thermocouples have been recognized as one swirl structure. Knowing the location of the particular thermocouples, schematic view of such flow structure inside the enclosure was drawn and shown in the Fig. 6. It should be emphasized that measurement points were in the distance of 5 mm from the front wall. That is why the drawn representation is shown in the plane and not in the whole volume. For the convection in a strong magnetic field (9 T) were seen few vortices, which might suggest slowing down of the flow.

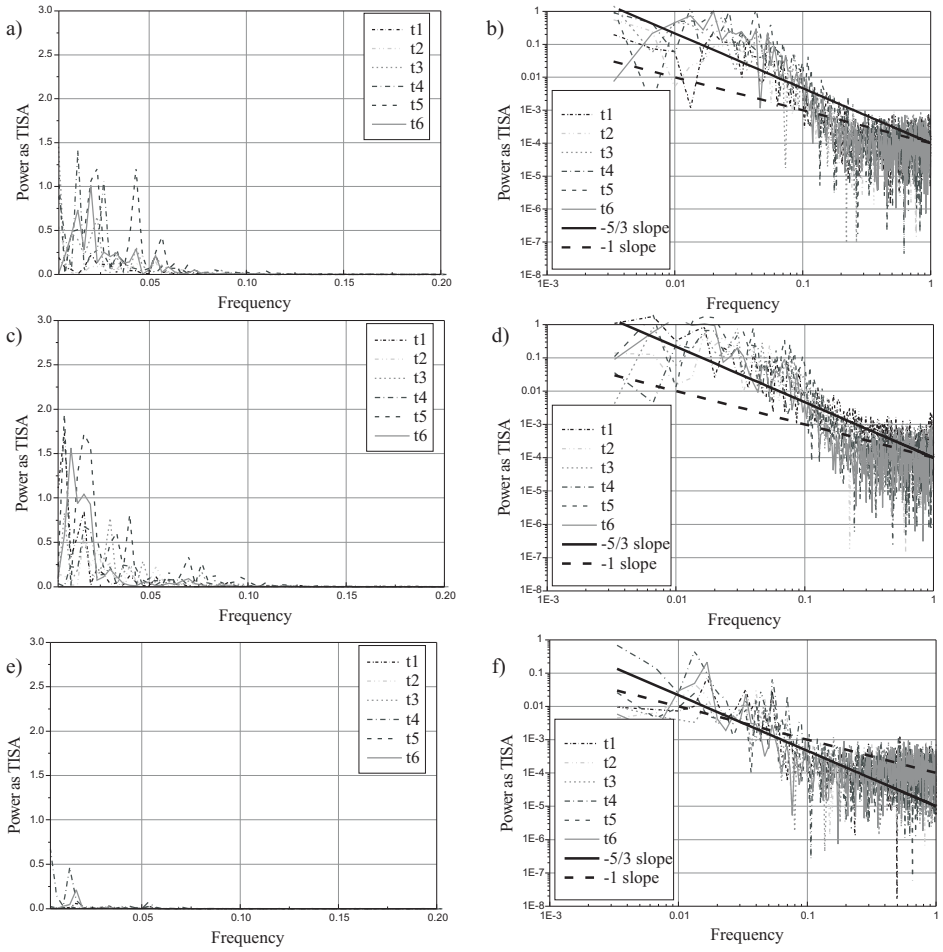

Figure 4: The power spectrum versus frequency without magnetic field for (a) Cu50, (c) Cu500, (e) Cu1000 and log-log scale representation for (b) Cu50, (d) Cu500, (f) Cu1000 nanofluids..

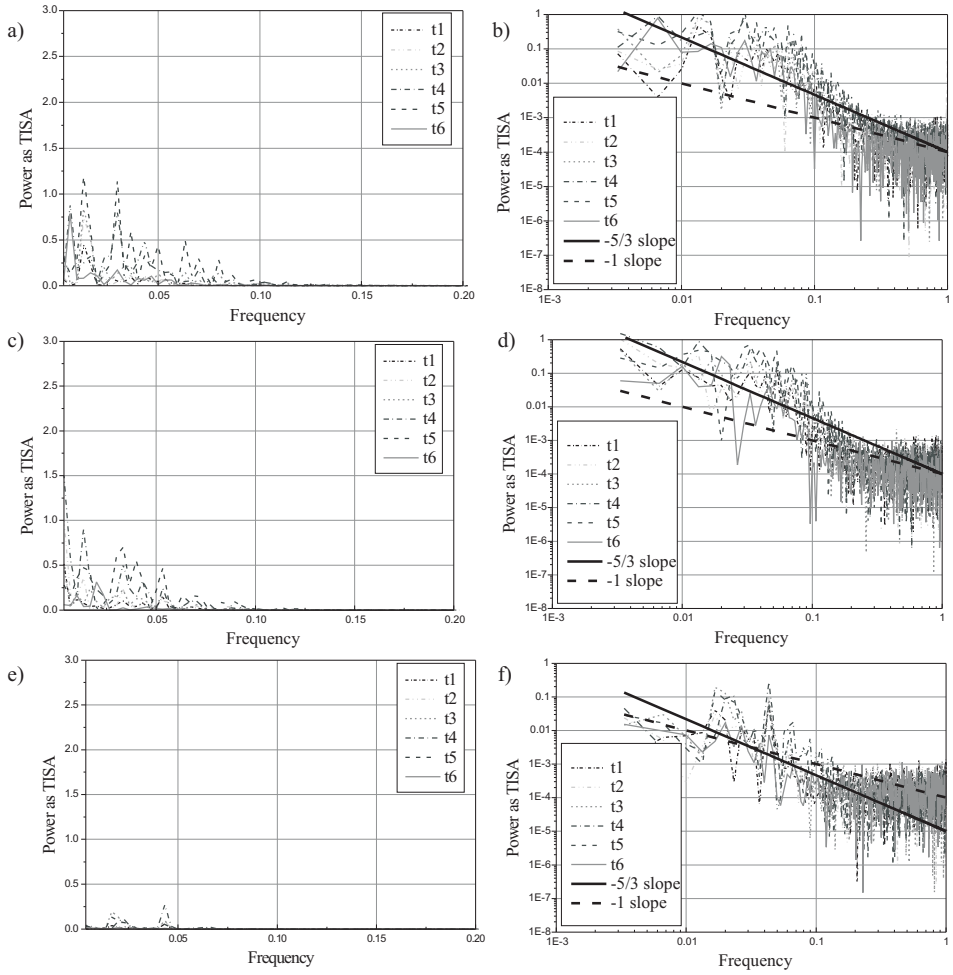

Figure 5: The power spectrum versus frequency at 9 T of magnetic field for (a) Cu50, (c) Cu500, (e) Cu1000 and log-log scale representation for (b) Cu50, (d) Cu500, (f) Cu1000 nanofluids.

4 Summary

The experimental analysis of thermomagnetic convection of 50, 500 and 1000 ppm concentrations copper nanofluids was presented. The impact of magnetic field on the transport processes and fluid flow structure for such low concentrations was investigated. Estimation of the heat transfer and flow structure was able due to the signal analysis.

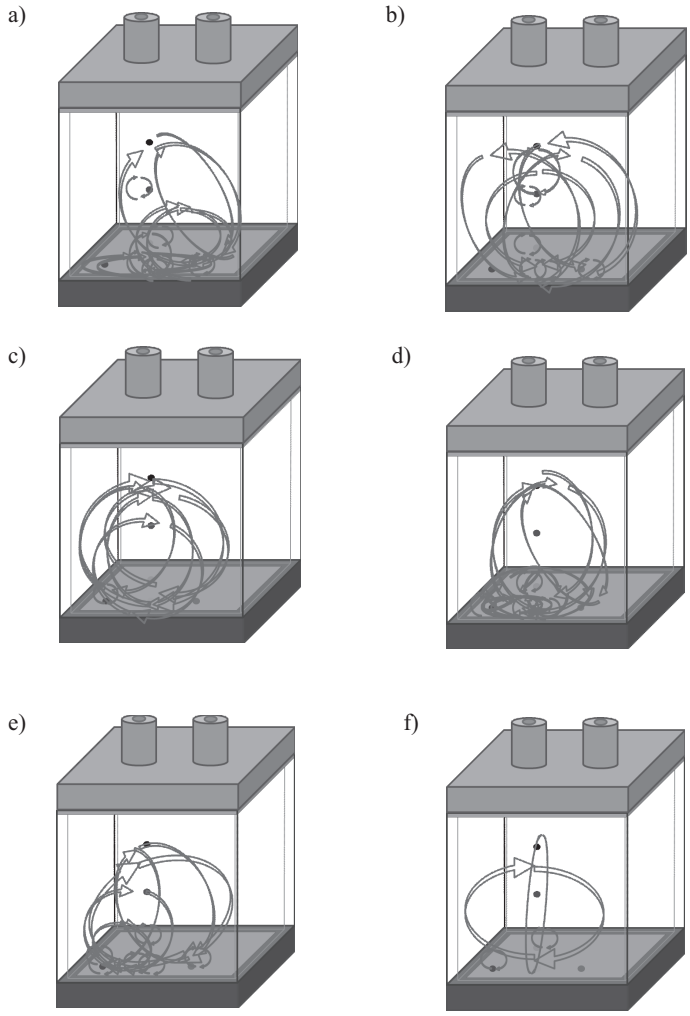

Figure 6: Schematic drawings showing structure of the vortices inside the enclosure without the magnetic field for nanofluids: a) Cu50, b) Cu500 and c) Cu1000, as well as with the magnetic induction equal to 9 T for: d) Cu50, e) Cu500, and f) Cu1000.

Reciprocal interaction between the gravitational and magnetic buoyancy forces affected the behavior of the fluid during the thermomagnetic convection. The magnetic buoyancy force was about 42–45% smaller than the gravitational buoyancy force, however it was able to increase the Nusselt number of about 25%.

Finally, it should be mentioned that few aspects of presented results still require a comprehensive clarification, among others, influence of higher nanoparticles concentration and magnetic field orientation on phenomena, distinguishing if the bulk flow governs the heat transfer or it depends on the particular components of nanofluid. Therefore, an overall understanding of this phenomenon, which will enable to draw the more general conclusions, needs complex analysis of the flow structure.

Acknowledgement The present work was supported by the Polish Ministry of Science Higher Educate(Grant AGH No. 15.11.210.307).

Received 10 April, 2015

References

[1] Yu W., Xie H.: *A review on nanofluids: Preparation, stability mechanisms, and applications.* J. Nanomater. **2012**(2012), 1–17.

[2] Khanafer K., Vafai K., Lightstone M.: *Buoyancy-driven heat transfer enhancement in a two-dimensional enclosure utilizing nanofluids.* Int. J. Heat Mass Transf. **46**(2003), 3639–3653.

[3] Abu-Nada E., Masoud Z., Oztop H.F., Campo A.: *Effect of nanofluid variable properties on natural convection in enclosures.* Int. J. Therm. Sci. **49**(2010), 479–491.

[4] Qi C., He Y., Yan S., Tian F., Hu Y.: *Numerical simulation of natural convection in a square enclosure filled with nanofluid using the two-phase Lattice Boltzmann method.* Nanoscale Res. Lett. **8**(2013), 56.

[5] Yang Y., Zhang Z.G., Grulke E.A., Anderson W.B., Wu G.: *Heat transfer properties of nanoparticle-in-fluid dispersions (nanofluids) in laminar flow.* Int. J. Heat Mass Transf. **48**(2005), 1107–1116.

[6] Li D., Xie W., Fang W.: *Preparation and properties of copper-oil-based nanofluids.* Nanoscale Res. Lett. **6**(2011), 373.

[7] Godson L., Raja B., Mohan Lal D., Wongwises S.: *Enhancement of heat transfer using nanofluids – An overview.* Renew. Sustain. Energy Rev. **14**(2010), 629–641.

[8] Ternik P., Rudolf R., Zunic Z.: *Numerical study of heat-transfer enhancement of homogeneous water-Au nanofluid under natural convection.* Mater. Technol. **46**(2012), 257–261.

[9] Barber J., Brutin D., Tadrist L.: *A review on boiling heat transfer enhancement with nanofluids.* Nanoscale Res. Lett. 6(2011), 280.

[10] Sheikholeslami M., Gorji Bandpy M., Ellahi R., Hassan M., Soleimani S.: *Effects of MHD on Cu-water nanofluid flow and heat transfer by means of CVFEM.* J. Magn. Magn. Mater. **349**(2014), 188–200.

[11] Gupta U., Ahuja J., Wanchoo R.K.: *Magneto convection in a nanofluid layer.* Int. J. Heat Mass Transf. **64**(2013), 1163–1171.

[12] Ghasemi B., Aminossadati S.M., Raisi A.: *Magnetic field effect on natural convection in a nanofluid-filled square enclosure.* Int. J. Therm. Sci. **50**(2011), 1748–1756.

[13] Roszko A., Fornalik-Wajs E., Donizak J., Wajs J., Kraszewska A., Pleskacz L.: *Magneto-thermal convection of low concentration nanofluids.* MATEC Web Conf. **6**(2014), 1–8.

[14] Wrobel W., Fornalik-Wajs E., Szmyd J.S.: *Experimental and numerical analysis of thermo-magnetic convection in a vertical annular enclosure.* Int. J. Heat Fluid Flow. **31**(2010), 1019–1031.

[15] Kenjeres S., Pyrda L., Wrobel W., Fornalik-Wajs E., Szmyd J.: *Oscillatory states in thermal convection of a paramagnetic fluid in a cubical enclosure subjected to a magnetic field gradient.* Phys. Rev. E. **85**(2012), 1–8.

[16] Mukherjee S., Paria S.: *Preparation and stability of nanofluids. A review.* IOSR-JMCE **9**(2013), 63–69.

[17] Xuan Y., Roetzel W.: *Conceptions for heat transfer correlation of nanofluids.* Int. J. Heat Mass Transf. **43**(2000), 3701–3707.

[18] Qi J., Wakayama N.I., Yabe A.: *Magnetic control of thermal convection in electrically non-conducting or low-conducting paramagnetic fluids.* Int. J. Heat Mass Transf. **44**(2001), 3043–3052.

[19] Sreenivasan K.R.: *The passive scalar spectrum and the Obukhov-Corrsin constant.* Phys. Fluids. **8**(1996), 189–196.

[20] Elsner J.W.: *Turbulence of Flows.* PWN, Warszawa 1989(in Polish).